

Simple adaptive control of seismically excited structures with MR dampers

F. Amini* and M. Javanbakht^a

Department of Civil Engineering, Iran University of Science and Technology, Tehran, Iran

(Received January 31, 2014, Revised April 17, 2014, Accepted May 27, 2014)

Abstract. In this paper, Simple Adaptive Control (SAC) method is used to mitigate the detrimental effects of earthquakes on MR-damper equipped structures. Acceleration Feedback (AF) is utilized since measuring the acceleration response of structures is known to be reliable and inexpensive. The SAC is simple, fast and as an adaptive control scheme, is immune against the effects of plant and environmental uncertainties. In the present study, in order to translate the desired control force into an applicable MR damper command voltage, a neural network inverse model is trained, validated and used through the simulations. The effectiveness of the proposed AF-based SAC control system is compared with optimal H₂/LQG controllers through numerical investigation of a three-story model building. The results indicate that the SAC controller is substantially effective and reliable in both undamaged and damaged structural states, specifically in reducing acceleration responses of seismically excited buildings.

Keywords: seismic control; acceleration feedback; simple adaptive control; MR dampers; neural networks

1. Introduction

Over the past four decades, the approach for improving the response of civil structures under natural hazards, such as earthquakes and strong winds, has been moving from conventional passive control systems to effective and smart active or semi-active systems (Casciati *et al.* 2012). While any of these systems have well-known merits and demerits, control strategies based on semi-active devices have allegedly combined the best features of both passive and active methods; namely, by offering the inherent reliability of passive systems and the adaptability and versatility of active systems (Casciati *et al.* 2012, Housner *et al.* 1997, Choi *et al.* 2004). In contrast with the active systems, a semi-active device does not require large power sources and therefore cannot inject mechanical energy into the controlled system, which results in inherent stabilizing behavior of such devices (Spencer Jr and Nagarajaiah 2003).

One of the most promising semi-active devices which belong to a family of controllable-fluid dampers is Magneto-Rheological (MR) damper. Having equipped with just one moving part, i.e. the piston, these dampers are mechanically simple and reliable. They use MR fluids which are able to reversibly change from a free-flowing linear viscous fluid to a semi-solid with controllable yield

*Corresponding author, Professor, E-mail: famini@iust.ac.ir

^aM.Sc. Graduate, E-mail: majd@inbox.com

strength when exposed to a magnetic field. As another merit of MR dampers, this process is so fast (i.e., it happens in milliseconds) and requires a low power which can be readily supplied by batteries (Housner *et al.* 1997, Bitaraf *et al.* 2010, Spencer Jr and Nagarajaiah 2003).

Extensive studies have been carried out on MR dampers both analytically and experimentally for large-scale as well as model prototypes (Rodriguez *et al.* 2009a, 2009b, Bahar *et al.* 2010). Due to highly non-linear characteristic of MR dampers, establishing a dynamic model to reflect their accurate behavior is rather challenging. Spencer *et al.* (1997a) have conducted a number of laboratory experiments and proposed a phenomenological model for MR dampers based on Bouc-Wen hysteresis model which has been widely used afterwards. Similar applications of Bouc-Wen model also have been reflected in literature (Domaneschi 2009, 2012). In addition, neural network model (Chang and Roschke 1998), fuzzy model (Schurter and Roschke 2000) and polynomial model (Choi *et al.* 2001) are also developed subsequently. Spencer Jr *et al.* (Spencer Jr *et al.* 1997b, Spencer Jr *et al.* 1998b) reported the design of a full-scale 20 ton MR damper and showed the capability of these devices for being used in practical civil engineering structures. In 2001, the first full-scale implementation of MR dampers for civil engineering applications was achieved in the Tokyo National Museum of Emerging Science and Innovation (Spencer Jr. and Nagarajaiah 2003). Implementation of these devices for bridge structures has been investigated in China (Chen *et al.* 2003, Li *et al.* 2007).

One of the challenges associated with the design and implementation of a control system with MR dampers, is determining the damper command voltage in order to produce the desired control force. Many proposed control algorithms modify the voltage by adopting on-off rules without taking into consideration any model for the MR damper behavior. These model-free strategies comprise clipped-optimal control, decentralized bang-bang control, control algorithm based on Lyapunov stability theory and modulated homogenous friction control (Dyke and Spencer Jr 1997, Ha *et al.* 2008). Another category of control methods based on an inverse model to provide required voltages also have been developed. Examples include inverse models based on neural networks (K-Karamodin and H-Kazemi 2010, Vadtala *et al.* 2013), fuzzy logic (Choi *et al.* 2004) and simplified mathematical inversions of MR damper phenomenological model (Tsang *et al.* 2006, Zhang *et al.* 2011, Bitaraf *et al.* 2010). Most recently, research studies have been conducted to develop appropriate models as well as control algorithms that better adapt to MR damper devices in order to improve dynamic structural responses (Casciati *et al.* 2012, Mohajer Rahbari *et al.* 2013).

The Simple Adaptive Control (SAC) method, as a type of Direct Model Reference Adaptive Control (DMRAC), was first introduced by Sobel *et al.* (1982) and further developed by the works of Bar-Kana and Kaufman (Bar-Kana and Kaufman 1985a, b, 1993, Kaufman *et al.* 1998), Bar-Kana (Bar-Kana 1987, 1991), Bar-Kana and Guez (1990) and Iwai *et al.* (Iwai and Mizumoto 1992, Iwai *et al.* 1993, Iwai and Mizumoto 1994, Iwai *et al.* 2006). The appealing advantages of SAC method with respect to other adaptive control methods include: (a) simplicity and speed, (b) applicability to large and complicated systems (e.g., non-minimum phase MIMO plants), (c) the ability to cope with internal uncertainties (e.g., unknown plant parameters and dynamics) and environmental disturbances and (d) successful experimental validation (Kaufman *et al.* 1998, Bitaraf and Hurlebaus 2013).

In this paper, the SAC method is adopted for seismic control of MR-damper equipped structure using limited AF. In the literature, AF control strategies for active control of seismically excited structures have been developed theoretically and experimentally (Spencer Jr *et al.* 1994, Dyke *et al.* 1996a, Dyke *et al.* 1996b, Jabbari *et al.* 1995). Due to reliability and cost-efficiency of absolute

acceleration measurement using accelerometers, this paper tends to provide a practical and reliable semi-active control scheme. A Neural Network Inverse Model (NNIM) for MR damper is also developed to translate the SAC control force into actual damper force. The effectiveness of the proposed system is studied and evaluated through the numerical investigation of a three-story model building presented by Dyke *et al.* (1996b).

2. Control algorithms

2.1 Simple Adaptive Control (SAC)

As a DMRAC scheme, SAC method was proposed by Sobel *et al.* (1982) as an attempt to make adaptive controllers simple. The “simple” here means that the method does not use identifiers or observers in its feedback loop and that the order of reference model can be much smaller than the order of controlled plant. This algorithm requires neither full state access nor prior knowledge of plant dynamics, but asymptotic stability requires the plant to satisfy Almost Strictly Positive Realness (ASPR) condition (Kaufman *et al.* 1998).

The controlled plant is represented by

$$\dot{x}_p = \mathbf{A}_p x_p + \mathbf{B}_p u_p + d_p \quad (1a)$$

$$y_p = \mathbf{C}_p x_p + \mathbf{D}_p u_p + d_0 \quad (1b)$$

where x_p is the plant state vector, u_p is the control input vector, y_p is the output vector and d_p and d_0 are plant and output disturbances, respectively.

For a plant represented by the triple $\{\mathbf{A}, \mathbf{B}, \mathbf{C}\}$ the ASPR condition holds when there exists a constant feedback gain \mathbf{K}_e (not needed for implementation) such that the transfer matrix

$$\mathbf{G}_s(s) = \mathbf{C}(s\mathbf{I} - \mathbf{A}_e)^{-1} \mathbf{B} \quad (2)$$

where $\mathbf{A}_e = \mathbf{A} + \mathbf{B}\mathbf{K}_e\mathbf{C}$, is Strictly Positive Real (SPR). The SPR condition holds if there exist two positive definite symmetric matrices, \mathbf{P} and \mathbf{Q} , such that the closed-loop system using \mathbf{K}_e satisfies simultaneously the following equations

$$\mathbf{P}(\mathbf{A} - \mathbf{B}\mathbf{K}_e\mathbf{C}) + (\mathbf{A} - \mathbf{B}\mathbf{K}_e\mathbf{C})^T \mathbf{P} = -\mathbf{Q} < 0 \quad (3a)$$

$$\mathbf{P}\mathbf{B} = \mathbf{C}^T \quad (3b)$$

The ASPR condition can be identified by some plant characteristics as (Bar-Kana 1991):

- (a) The plant is minimum-phase (i.e., all zeros have negative real parts)
- (b) The product $\mathbf{C}\times\mathbf{B}$ is positive definite

The ASPR condition for proper systems $\{\mathbf{A}, \mathbf{B}, \mathbf{C}, \mathbf{D}\}$ also can be declared as:

- (a) The plant is minimum-phase
- (b) The \mathbf{D} is positive definite

Whenever the acceleration feedback is used, the plant is not strictly proper (i.e., $\mathbf{D}\neq\mathbf{0}$) and the product $\mathbf{C}\times\mathbf{B}$ is not positive definite; thus the ASPR condition does not hold; however, due to inherent stability of MR damper system the plant must be able to be satisfactorily controlled despite mentioned limitation, which has to be verified through simulations.

The plant output y_p must track the output of a desired well-behaved reference model

$$\dot{x}_m = \mathbf{A}_m x_m + \mathbf{B}_m u_m \quad (4-a)$$

$$y_m = \mathbf{C}_m x_m + \mathbf{D}_m u_m \quad (4-b)$$

where x_m is the model state vector, u_m is the command input vector and y_m is the model output vector. Defining an appropriate reference model that always behaves better than the plant is an important part of the SAC method.

Then the measured tracking error

$$e_y(t) = y_m(t) - y_p(t) \quad (5)$$

has to be minimized by the adaptive control system. The control command is then calculated by

$$u_p(t) = \mathbf{K}(t)r(t) \quad (6)$$

where

$$\mathbf{K}(t) = \mathbf{K}_p(t) + \mathbf{K}_I(t) \quad (7)$$

$$r(t) = \begin{bmatrix} e_y^T(t) & x_m^T(t) & u_m^T(t) \end{bmatrix}^T \quad (8)$$

The proportional and integral terms of adaptive gain $\mathbf{K}(t)$ are calculated as

$$\mathbf{K}_p(t) = e_y(t)r^T(t)\bar{\mathbf{T}} \quad (9)$$

$$\dot{\mathbf{K}}_I(t) = e_y(t)r^T(t)\mathbf{T} - \sigma \mathbf{K}_I(t) \quad (10)$$

where the positive definite matrices $\bar{\mathbf{T}}$ and \mathbf{T} and the positive value σ are design parameters of SAC algorithm and should be tuned by the designer (Bar-Kana and Kaufman 1988). The block diagram of SAC method is shown in Fig. 1.

2.2 H_2/LQG optimal control

A type of clipped-optimal controller based on AF has been proposed by Dyke *et al.* (1996b). The approach is to design a linear optimal controller $\mathbf{K}_c(s)$ that provides a desired control force f_c based on measured responses y and measured damper force f . Due to stochastic nature of seismic ground motions, experimentally-verified H_2/LQG strategies may be used to obtain the controller $\mathbf{K}_c(s)$. The desired control force is: ($L\{\cdot\}$ is Laplace transform)

$$f_c = L^{-1} \left\{ -\mathbf{K}_c(s)L \begin{bmatrix} y \\ f \end{bmatrix} \right\} \quad (11)$$

The state-space form of the controller $\mathbf{K}_c(s)$ is represented by

$$\dot{\hat{x}} = (\mathbf{A} - \mathbf{L}\mathbf{C})\hat{x} + [\mathbf{L} \quad \mathbf{B} - \mathbf{L}\mathbf{D}] \begin{bmatrix} y \\ f \end{bmatrix} \quad (12-a)$$

$$f_c = -\mathbf{K} \hat{x} \quad (12-b)$$

where \hat{x} is the estimated state vector using Kalman filter, matrix \mathbf{L} is the observer gain matrix for

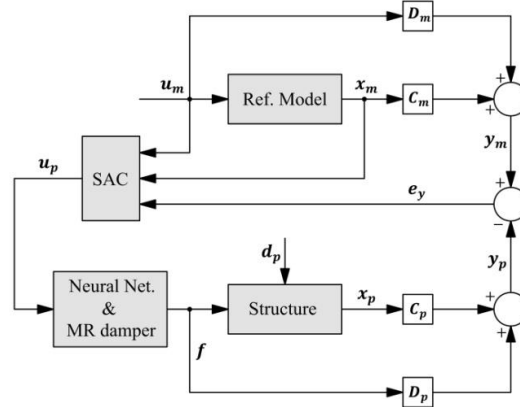


Fig. 1 Block diagram of SAC method for MR-damper equipped structure

LQG (Linear Quadratic Gaussian), matrix K is the optimal gain matrix for LQR (Linear Quadratic Regulator) and A , K , C and D are plant state-space matrices. The L and K matrices can be calculated using MATLAB via *kalman.m* and *lqr.m* functions, respectively.

The regulator is designed such that the cost function: (E denotes expected value)

$$J = E \left\{ \lim_{\tau \rightarrow \infty} \frac{1}{\tau} \int_0^{\tau} [(Cz)^T Q(Cz) + rf_c^2] dt \right\} \quad (13)$$

is minimized and the weighting matrix Q and r are appropriately selected to get the best results.

2.3 Clipping algorithms

The command voltage v of MR damper is the only parameter that can be directly controlled to produce the desired control force. When no inverse model is considered for MR damper, clipping algorithms may be utilized to translate required control force into a voltage input. Several clipping approaches have been proposed in the literature (Dyke *et al.* 1996b, Yoshida and Dyke 2004, Purohit and Chandiramani 2011). In the original clipping algorithm (Dyke *et al.* 1996b), the optimal force is compared to the damper force and the command voltage is then calculated by

$$v_i = V_{\max} H \{ (f_{LQG} - f_{mr}) f_{mr} \} \quad (14)$$

where V_{\max} is the saturation voltage of MR damper and $H\{\cdot\}$ is the Heaviside step function.

A modified version of this clipping algorithm has been subsequently proposed in (Yoshida and Dyke 2004) where a linear relationship between the applied voltage and the maximum damper force f_{mr}^{\max} is considered and the command voltage is then calculated by

$$v_i = V_{ci} H \{ (f_{LQG} - f_{mr}) f_{mr} \} \quad (15)$$

and

$$V_{ci} = \begin{cases} V_{\max} (f_{LQG} / f_{mr}^{\max}) & f_{LQG} \leq f_{mr}^{\max} \\ V_{\max} & f_{LQG} > f_{mr}^{\max} \end{cases} \quad (16)$$

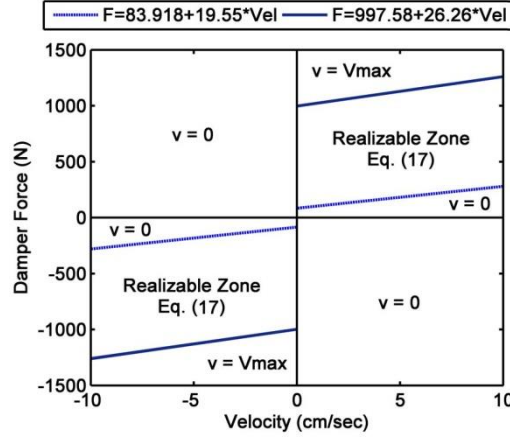


Fig. 2 Realizable MR damper force zone in first and third quadrant of $f-\dot{x}$ plane (Purohit and Chandiramani 2011)

Recently, Purohit and Chandiramani (2011) have proposed a new algorithm based on realizable region of MR damper force and velocity that is named Inverse Quadratic Voltage Law (IQVL). In their work, a MR damper similar to the present study has been used and the realizable zone is defined graphically as shown in Fig. 2. Further, in the realizable zone, the inverse relation between damper force and voltage is approximately governed by the following quadratic equation

$$\Phi v^2 + \Psi v + \Omega = 0 \quad (17)$$

where (\dot{x} denotes damper velocity)

$$\Phi = c_{1b}\alpha_b z_u + c_{1b}c_{0b}\dot{x} \quad (18a)$$

$$\Psi = (c_{1a}\alpha_b + c_{1b}\alpha_a)z_u + (c_{1a}c_{0b} + c_{1b}c_{0a})\dot{x} - (c_{0b} + c_{1b})f_{mr} \quad (18b)$$

$$\Omega = c_{1a}\alpha_a z_u + c_{1a}c_{0a}\dot{x} - (c_{0a} + c_{1a})f_{mr} \quad (18c)$$

$$z_u = \pm \left(\frac{A}{\gamma + \beta} \right)^{1/n} \quad (18d)$$

and z_u is positive in first quadrant and negative in third quadrant. In addition to MR damper force, this algorithm requires the measurement of damper velocity.

3. System dynamics

3.1 MR damper dynamics

The phenomenological model of MR damper is introduced by Spencer *et al.* (1997a) based on the response of a prototype MR damper through experimental studies. Fig. 3 illustrates the mechanical idealization of MR damper based on a Bouc-Wen hysteresis model which is governed

by the following simultaneous non-linear equations

$$F = c_1 \dot{y} + k_1 (x - x_0) \quad (19)$$

$$\dot{y} = \frac{1}{(c_0 + c_1)} \{ \alpha z + c_0 \dot{x} + k_0 (x - y) \} \quad (20)$$

$$\dot{z} = -\gamma |\dot{x} - \dot{y}| z |z|^{n-1} - \beta (\dot{x} - \dot{y}) |z|^n + A (\dot{x} - \dot{y}) \quad (21)$$

where F , x and \dot{x} are damper force, displacement and velocity, respectively; k_1 is the accumulator stiffness with the initial displacement of x_0 ; k_0 is used to emulate the stiffness at large velocities; c_0 is the observed viscous damping at large velocities; c_1 is included to produce the observed roll-off at low velocities; z is an evolutionary variable that describes the hysteretic characteristic of MR damper; γ and β affect the shape and A affects the slope of hysteresis loop, while n governs the smoothness of linear to non-linear transition (Purohit and Chandiramani 2011).

The voltage-dependent model parameters are given by the following equations

$$\alpha = \alpha_a + \alpha_b u \quad (22)$$

$$c_1 = c_{1a} + c_{1b} u \quad (23)$$

$$c_0 = c_{0a} + c_{0b} u \quad (24)$$

$$\dot{u} = -\eta (u - v) \quad (25)$$

where Eq. (25) is a first order filter to account for the dynamics of rheological equilibrium of MR fluid and v is the command voltage sent to current driver. A total of 14 parameters for a prototype MR damper have been determined using constrained non-linear optimization of experimental data (Spencer *et al.* 1997a) and are given in Table 1. The saturation voltage for this prototype is reported as 2.25 V. The above model estimates the MR damper force based on three parameters, namely: (a) damper displacement, (b) damper velocity and (c) command voltage.

In order to convert the required control force determined by SAC controller to the voltage, an inverse model of MR damper is indispensable. Due to the inherent non-linear characteristics of MR damper, it is challenging to obtain an analytical inverse model. In order to tackle this challenge, a feed-forward back-propagation neural network model has been suggested (Vadtala *et al.* 2013, K-Karamodin and H-Kazemi 2010).

Table 1 Parameters for the prototype 1000 N MR damper

Parameter	Value	Parameter	Value
c_{0a}	21.0 N.sec/cm	α_a	140 N/cm
c_{0b}	3.50 N.sec/cm.V	α_b	695 N/cm.V
c_{1a}	283 N.sec/cm	γ	363 cm ⁻²
c_{1b}	2.95 N.sec/cm.V	β	363 cm ⁻²
k_0	46.9 N/cm	A	301
k_1	5.00 N/cm	n	2
x_0	14.3 cm	η	190 sec ⁻¹

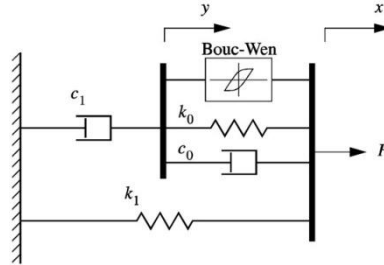


Fig. 3 The mechanical model of the MR damper

A similar neural network architecture as the one proposed by K-Karamodin and H-Kazemi (2010) is adopted here that comprises two hidden layers and gets trained based on current and few (e.g., three) previous histories of randomly generated data of displacement, velocity and voltage (Fig. 4). The MR damper parameters, given in Table 1, are used for network training except that x_0 is set to zero in order to revoke initial offset caused by damper's accumulator (Dyke *et al.* 1996b).

3.2 Structural dynamics

In this study, the model of a three-story shear building equipped with a rigidly-connected MR damper between the ground and the first floor of the structure is considered (Fig. 5). The motion of the structure in linear region is governed by the following equation

$$\mathbf{M} \ddot{\mathbf{x}} + \mathbf{C} \dot{\mathbf{x}} + \mathbf{K} \mathbf{x} = \mathbf{\Gamma} f - \mathbf{M} \Lambda \ddot{x}_g \quad (26)$$

where \mathbf{M} , \mathbf{C} and \mathbf{K} are mass, damping and stiffness matrices, respectively; $\mathbf{\Gamma}$ is the location matrix of MR dampers; f is the applied control force defined by Eq. (19); Λ is a column vector of ones; \ddot{x}_g is the one-dimensional ground acceleration and \mathbf{x} is a vector of relative displacement of stories relative to ground.

The structural measurements used in the proposed controller to generate the desired control force comprise only the absolute acceleration of the first floor. However, the displacement of MR damper which is equal to that of the first floor is also indispensable for damper force evaluation. Rewriting Eq. (26) in state-space form gives

$$\dot{\mathbf{z}} = \mathbf{A} \mathbf{z} + \mathbf{B} f + \mathbf{E} \ddot{x}_g \quad (27a)$$

$$y = \mathbf{C} \mathbf{z} + \mathbf{D} f + d \quad (27b)$$

$$\text{where } \mathbf{z} = \begin{bmatrix} \mathbf{x} \\ \dot{\mathbf{x}} \end{bmatrix}_{2n \times 1}; \quad \mathbf{A} = \begin{bmatrix} \mathbf{0}_{n \times n} & \mathbf{I}_{n \times n} \\ -\mathbf{M}^{-1} \mathbf{K} & -\mathbf{M}^{-1} \mathbf{C} \end{bmatrix}_{2n \times 2n}; \quad \mathbf{B} = \begin{bmatrix} \mathbf{0}_{n \times r} \\ \mathbf{M}^{-1} \mathbf{\Gamma} \end{bmatrix}_{2n \times r}; \quad \mathbf{E} = \begin{bmatrix} \mathbf{0}_{n \times 1} \\ -\Lambda \end{bmatrix}_{2n \times 1}$$

$$\mathbf{C} = \mathbf{G} \times \begin{bmatrix} -\mathbf{M}^{-1} \mathbf{K} & -\mathbf{M}^{-1} \mathbf{C} \\ 1 & 0 & 0 & 0 \end{bmatrix}_{(n+r) \times 2n}; \quad \mathbf{D} = \mathbf{G} \times \begin{bmatrix} \mathbf{M}^{-1} \mathbf{\Gamma} \\ 0 \end{bmatrix}_{(n+2r) \times 1}; \quad \mathbf{G} = \begin{bmatrix} 1 & 0 & 0 & 0 \\ 0 & 0 & 0 & 1 \end{bmatrix}_{p \times (n+r)}$$

where n =number of degrees of freedom, r =number of control forces, p =number of outputs and d is measurement noise which is neglected in this study.

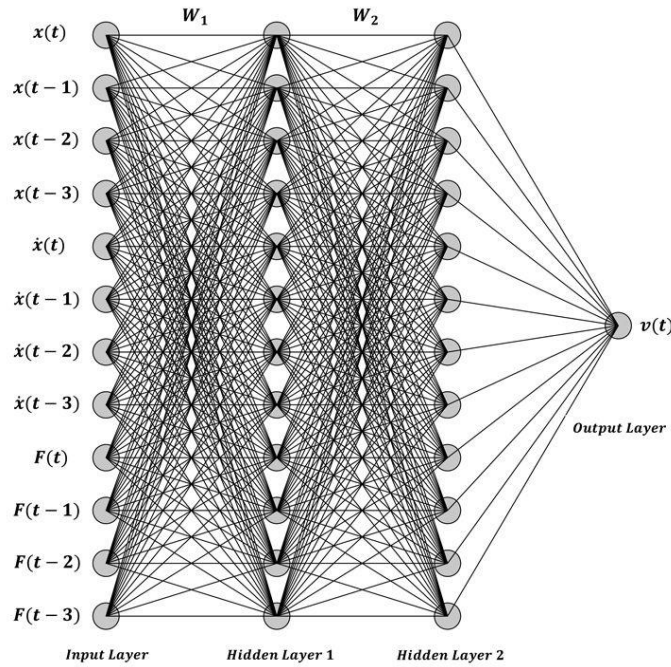


Fig. 4 NNIM for MR damper; $x(t-i)$ refers to displacement record at previous i^{th} time step, etc

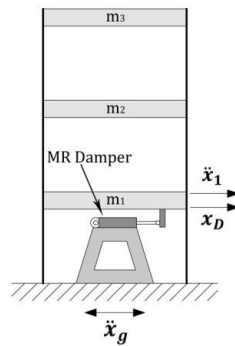


Fig. 5 Three-story model building equipped with the MR damper

4. Numerical example

To evaluate the performance of the proposed AF-based SAC controller, the three-story building (Fig. 5) is numerically studied. Responses of the SAC-controlled structure are then compared to those of the uncontrolled system, passive-on system (i.e., command voltage to MR damper is held at the saturation value: V_{max}) and two optimal controllers.

The system matrices are given as: (Dyke *et al.* 1996b)

$$M = \begin{bmatrix} 98.3 & 0 & 0 \\ 0 & 98.3 & 0 \\ 0 & 0 & 98.3 \end{bmatrix} \text{ kg}; C = \begin{bmatrix} 175 & -50 & 0 \\ -50 & 100 & -50 \\ 0 & -50 & 50 \end{bmatrix} \text{ N.sec/m}$$

Table 2 Earthquake records used in numerical study

Earthquake name and date	Station and component	PGA (m/sec ²)
Imperial Valley (1940)	El Centro (N-S)	3.417
Takochi-oki (1968)	Hachinohe (N-S)	2.25
Northridge (1994)	Sylmar County (N-S)	8.268
Kobe (1995)	KJMA (N-S)	8.178

$$\mathbf{K} = \begin{bmatrix} 12 & -6.84 & 0 \\ -6.84 & 13.7 & -6.84 \\ 0 & -6.84 & 6.84 \end{bmatrix} \times 10^5 \text{ N/m}; \Gamma = [-1 \ 0 \ 0]^T; \Lambda = [1 \ 1 \ 1]^T$$

and MR damper parameters given in Table 1 are used in numerical study except for $x_0=0$.

Four earthquake records are studied in the simulations (Table 2) and as suggested in (Dyke *et al.* 1996b), because the considered building is a scaled model, the earthquakes are reproduced at five times the original recorded rate, i.e., time scale of 0.2 is applied. Three magnification factors of Peak Ground Acceleration (PGA) are considered (i.e., MF=0.5, 1 and 1.5) for each record. Since the significant aftershocks may occur soon after the main earthquake, the impact of degradation should not preferably affect the desired control performance. In order to evaluate this matter, a 20% reduction in stiffness matrix (i.e., 10% increase in fundamental period, approximately) is applied as a potential damage effect and the results are evaluated for both pre-earthquake and post-earthquake structures.

In SAC method, the reference model exhibits the desired behavior which should be tracked by controlled plant. Although the order of reference model is allowed to be smaller than the order of plant, the output orders should be the same since y_p tracks y_{mp} . Defining an appropriate reference model that always behaves better than the plant is an important part of the SAC algorithm. In this study, the reference model is chosen as a 2-DOF shear building with the system matrices given below

$$\mathbf{M}_m = \begin{bmatrix} 1 & 0 \\ 0 & 1 \end{bmatrix} \text{ kg}; \mathbf{K}_m = \begin{bmatrix} 2 & -1 \\ -1 & 1 \end{bmatrix} \times 10^5 \text{ N/m}; \zeta_m = 10\% \text{ (for all modes)}$$

where the acceleration of the first floor is taken as y_m .

The reference model has been designed through several iterations such that the high damping ratio guarantees the desired behavior of reference model. For the worst case of the all ground motion records which are considered in the simulations, the maximum relative displacement of the reference model is less than 4% in contrast with the uncontrolled plant and the maximum absolute acceleration of the reference model is less than 73% of the uncontrolled plant peak acceleration. The reference model must be chosen such that it fits to safety and serviceability requirements of acceleration and displacement responses. Fig. 6 compares the first story response histories of the reference model, uncontrolled structure and SAC controller for El Centro earthquake (MF=1), which shows the plant's perfect model tracking.

In order to increase the compatibility level of controller to ground motion characteristics, command input u_m is chosen to be the earthquake input applied to the structure which is monitored via an accelerometer. The SAC parameters are set through iterations to get the best results as:

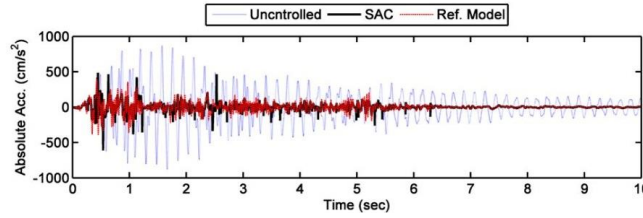


Fig. 6 Comparison of the first story response histories of reference model, SAC controller and uncontrolled structure under El Centro earthquake (MF=1)

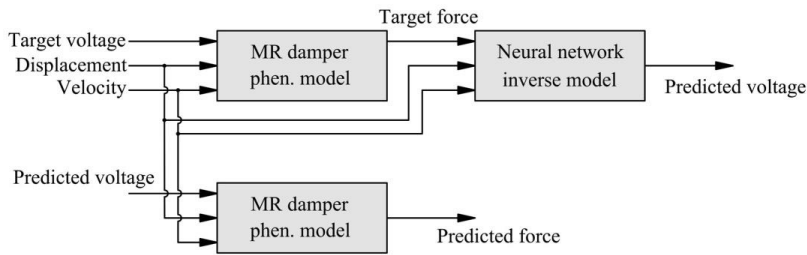


Fig. 7 The validation process of trained NNIM

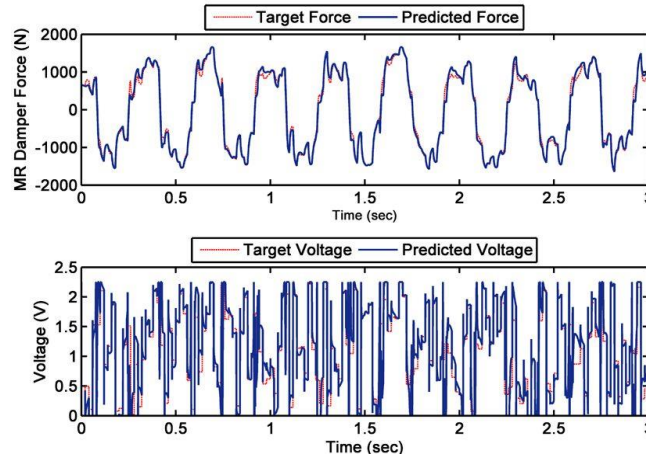


Fig. 8 Validation of trained NNIM for a 3 Hz sinusoidal displacement with an amplitude of 1.5 cm and randomly generated target voltage

$$\bar{T} = \text{diag}([1.711111]) \times 10^2; T = I_{6 \times 6}; \sigma = 0.01$$

For LQG algorithm, as described in (Dyke *et al.* 1996b), the best results were obtained by using $r=10^{-17}$ and choosing all the elements of the weighting matrix $Q_{4 \times 4}$ zero except for $Q_{3 \times 3}=1$. In designing the controller, the measurement noise is assumed to be identically distributed, statistically independent Gaussian white noise processes and $S_{\ddot{x}_g \ddot{x}_g} / S_{v_i v_i} = 50$ (i.e., $E(d_p d_p^T) = 50, E(d_o d_o^T) = I_m$; where m is the number of outputs).

Table 3 Summary of the first nine evaluation criteria for the benchmark problem

Floor Displacement	Inter story drift	Floor Acceleration	Base Shear
$J_1 = \frac{\max x_i(t) }{x^{max}}$	$J_2 = \frac{\max(d_i(t)/h_i)}{d^{max}}$	$J_3 = \frac{\max \ddot{x}_i(t) }{\ddot{x}^{max}}$	$J_4 = \frac{\max \sum_i m_i \ddot{x}_i(t) }{F_b^{max}}$
Normed Floor Displacement	Normed Inter story drift	Normed Floor Acceleration	Normed Base Shear
$J_5 = \frac{\max\ x_i(t)\ }{\ x^{max}\ }$	$J_6 = \frac{\max\ d_i(t)/h_i\ }{\ d^{max}\ }$	$J_7 = \frac{\max\ \ddot{x}_i(t)\ }{\ \ddot{x}^{max}\ }$	$J_8 = \frac{\ \sum_i m_i \ddot{x}_i(t)\ }{\ F_b^{max}\ }$
Control Force			
$J_9 = \frac{\max f_i(t) }{W}$			

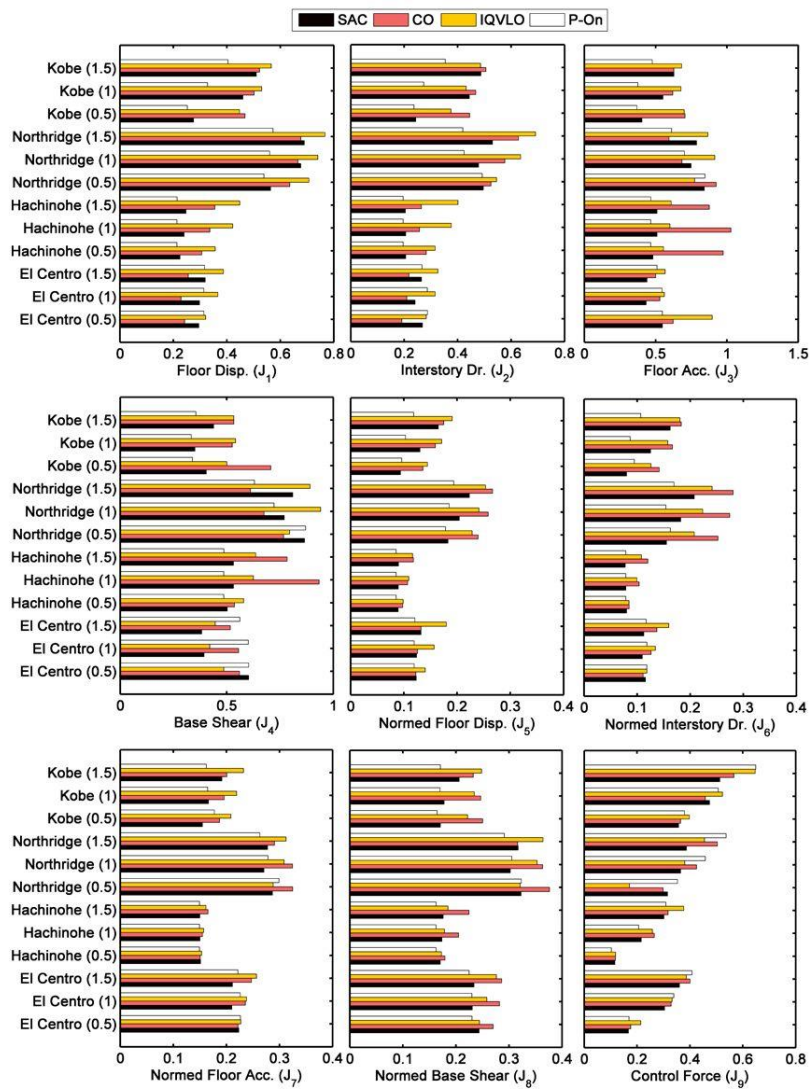


Fig. 9 Evaluation criteria for the undamaged structure controlled via SAC, CO, IQVLO and Passive-on

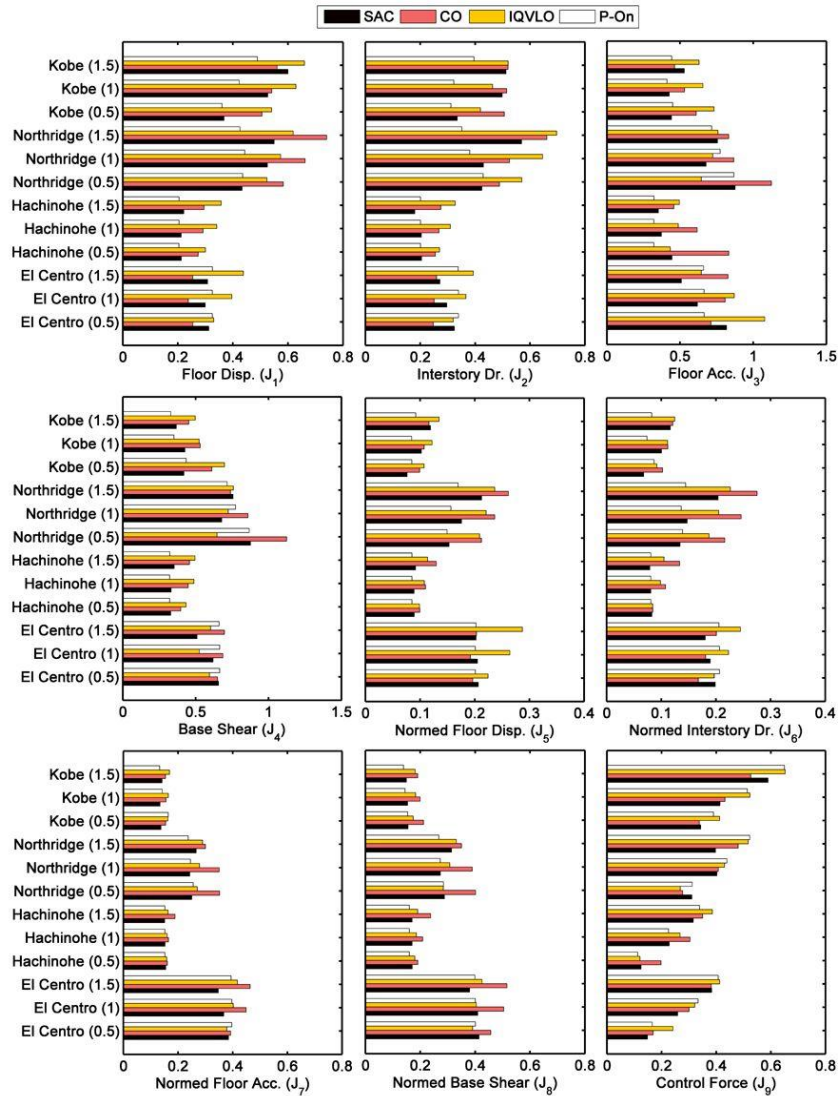


Fig. 10 Evaluation criteria for the damaged structure controlled via SAC, CO, IQVLO and Passive-on

The validation process of NNIM is carried out using a flowchart shown in Fig. 7 (Zong *et al.* 2012) and the results confirm that the predicted voltages and forces track the target ones suitably well (Fig. 8).

Among the previously described optimal algorithms, Clipped-Optimal and IQVL-Optimal are considered here for comparing purposes and are referred to here as CO and IQVLO, respectively. As reported by (Purohit and Chandiramani 2011), IQVLO illustrates better performance when the Eq. (17) is substituted with the constant maximum voltage V_{max} and therefore Eq. (17) is neglected in the simulations.

Different evaluation criteria sets have been used in structural control studies to compare the performance of competitive control approaches. In this study, the first nine criteria defined in

benchmark problem (Spencer Jr. *et al.* 1998a) is used in which J_1 to J_9 stands for the criterion of floor displacement, inter story drift, floor acceleration, base shear, normed floor displacement, normed inter story drift, normed floor acceleration, normed base shear and control force, respectively (Table 3). Sufficient simulation time must be considered in order to compute normed criteria.

Figs. 9-10 summarize the calculated evaluation criteria for different control strategies and different types of ground motion (e.g., both far-field: El Centro and Hachinohe, and near-fault: Northridge and Kobe, with different intensities) for undamaged and damaged structure, respectively.

Although a less number of output measurements are used in SAC in contrast with CO and IQVO, and despite the simplicity of its structure, it shows to be efficient in both pre-earthquake and post-earthquake situations, specifically in reducing acceleration responses (J_3). The SAC's independency of plant parameters is verified through the post-earthquake evaluation as can be seen in Fig. 10. In almost all the cases, the SAC does not exhibit a worse behavior than other controllers while producing smaller control force as suggested by J_9 criterion. The evaluation criteria suggest that the reference model and SAC parameters are selected appropriately and that the non-ASPR plant is suitably controlled via AF-based SAC method.

5. Conclusions

In order to provide a practical semi-active control system, in this study, a simple adaptive controller using AF is proposed to enhance the seismic response of a MR-damper equipped building. Numerical simulations are conducted to investigate the performance and superiority of the proposed control scheme for both pre- and post-earthquake structures under the effect of different ground motions. As the results indicate, compared to the optimal H_2/LQG controllers, the SAC shows very desirable and efficient control performance even by using fewer output feedbacks. In almost all the simulation cases, the SAC exhibits a satisfactory result in contrast with the other controllers while producing smaller control forces. Another advantage of using the SAC method for a semi-active control scheme, which is verified through the simulations, is the inherent stability of such systems that allows the designer to tackle non-ASPR plants especially as the case of AF-based controller (where $D \neq 0$ and $C \times B < 0$). By combining AF which utilizes cost-effective and reliable sensors and the proposed SAC control algorithm, this research aims at proposing an applicable semi-active control system.

References

- Bahar, A., Pozo, F., Acho, L., Rodellar, J. and Barbat, A. (2010), "Parameter identification of large-scale magnetorheological dampers in a benchmark building", *Comput. Struct.*, **88**(3-4), 198-206.
- Bar-Kana, I. and Kaufman, H. (1985a), "Global stability and performance of a simplified adaptive algorithm", *Int. J. Control*, **42**(6), 1491-1505.
- Bar-Kana, I. and Kaufman, H. (1985b), "Robust simplified adaptive control for a class of multivariable continuous-time systems", *24th IEEE Conference on Decision and Control*.
- Bar-Kana, I. (1987), "Parallel feedforward and simplified adaptive control", *Int. J. Adap. Control Sig. Pr.*, **1**(2), 95-109.
- Bar-Kana, I. and Kaufman, H. (1988), "Simple adaptive control of uncertain systems", *Int. J. Adap. Control*

- Sig. Pr.*, **2**(2), 133-143.
- Bar-Kana, I. and Guez, A. (1990), "Simple adaptive control for a class of non-linear systems with application to robotics", *Int. J. Control*, **52**(1), 77-99.
- Bar-Kana, I. (1991), "Positive-realness in multivariable stationary linear systems", *J. Franklin Inst.*, **328**(4), 403-417.
- Bar-Kana, I. and Kaufman, H. (1993), "Simple adaptive control of large flexible space structures", *IEEE Tran. Aerosp. Elec. Syst.*, **29**(4), 1137-1149.
- Bitaraf, M., Ozbulut, O.E., Hurlebaus, S. and Barroso, L. (2010), "Application of semi-active control strategies for seismic protection of buildings with MR dampers", *Eng. Struct.*, **32**(10), 3040-3047.
- Bitaraf, M. and Hurlebaus, S. (2013), "Semi-active adaptive control of seismically excited 20-story nonlinear building", *Eng. Struct.*, **56**, 2107-2118.
- Casciati, F., Rodellar, J. and Yildirim, U. (2012), "Active and semi-active control of structures - theory and applications: A review of recent advances", *J. Intel. Mater. Syst. Struct.*, **23**(11), 1181-1195.
- Chang, C. and Roschke, P. (1998), "Neural network modeling of a magnetorheological damper", *J. Intel. Mater. Syst. Struct.*, **9**(9), 755-764.
- Chen, Z., Wang, X., Ko, J., Ni, Y., Spencer Jr, B.F. and Yang, G. (2003), "MR damping system on Dongting Lake cable-stayed bridge", *Society of Photo-Optical Instrumentation Engineers (SPIE) Conference Series*.
- Choi, K.M., Cho, S.W., Jung, H.J. and Lee, I.W. (2004), "Semi-active fuzzy control for seismic response reduction using magnetorheological dampers", *Earthq. Eng. Struct. Dyn.*, **33**(6), 723-736.
- Choi, S., Lee, S. and Park, Y. (2001), "A hysteresis model for the field-dependent damping force of a magnetorheological damper", *J. Sound Vib.*, **245**(2), 375-383.
- Domaneschi, M. (2009), "Feasible control solutions of the ASCE benchmark cable-stayed bridge", *Struct. Control Hlth. Monit.*, **17**(6), 675-693
- Domaneschi, M. (2012), "Simulation of controlled hysteresis by the semi-active Bouc-Wen model", *Comput. Struct.*, **106-107**, 245-257
- Dyke, S., Spencer Jr, B., Quast, P., Sain, M., Jr, D.K. and Soong, T. (1996a), "Acceleration feedback control of MDOF structures", *J. Eng. Mech.*, **122**(9), 907-918.
- Dyke, S., Spencer Jr, B., Sain, M. and Carlson, J. (1996b), "Modeling and control of magnetorheological dampers for seismic response reduction", *Smart Mater. Struct.*, **5**(5), 565.
- Dyke, S. and Spencer Jr, B. (1997), "A comparison of semi-active control strategies for the MR damper", *Proceedings of the Intelligent Information Systems, IIS'97*.
- Ha, Q.P., Kwok, N.M., Nguyen, M.T., Li, J. and Samali, B. (2008), "Mitigation of seismic responses on building structures using MR dampers with Lyapunov-based control", *Struct. Control Hlth. Monit.*, **15**(4), 604-621.
- Housner, G.W., Bergman, L.A., Caughey, T., Chassiakos, A., Claus, R., Masri, S., Skelton, R., Soong, T., Spencer, B. and Yao, J.T. (1997), "Structural control: past, present, and future", *J. Eng. Mech.*, **123**(9), 897-971.
- Iwai, Z. and Mizumoto, I. (1992), "Robust and simple adaptive control systems", *Int. J. Control*, **55**(6), 1453-1470.
- Iwai, Z., Mizumoto, I. and Ohtsuka, H. (1993), "Robust and simple adaptive control system design", *Int. J. Adap. Control Sig. Pr.*, **7**(3), 163-181.
- Iwai, Z. and Mizumoto, I. (1994), "Realization of simple adaptive control by using parallel feedforward compensator", *Int. J. Control*, **59**(6), 1543-1565.
- Iwai, Z., Mizumoto, I. and Nakashima, Y. (2006), "Multivariable stable PID controller design with parallel feedforward compensator", *SICE-ICASE, 2006, International Joint Conference*.
- Jabbari, F., Schmitendorf, W. and Yang, J. (1995), " H_∞ control for seismic-excited buildings with acceleration feedback", *J. Eng. Mech.*, **121**(9), 994-1002.
- K-Karamodin, A. and H-Kazemi, H. (2010), "Semi-active control of structures using neuro-predictive algorithm for MR dampers", *Struct. Control Hlth. Monit.*, **17**(3), 237-253.
- Kaufman, H., Bar-Kana, I. and Sobel, K. (1998), *Direct Adaptive Control Algorithms: Theory and Applications*, Springer, New York, NY, USA.

- Li, H., Liu, M., Li, J., Guan, X. and Ou, J. (2007), "Vibration control of stay cables of the shandong binzhou yellow river highway bridge using magnetorheological fluid dampers", *J. Bridge Eng.*, **12**(4), 401-409.
- Mohajer Rahbari, N., Farahmand Azar, B., Talatahari, S. and Safari, H. (2013), "Semi-active direct control method for seismic alleviation of structures using MR dampers", *Struct. Control Hlth. Monit.*, **20**(6), 1021-1042.
- Purohit, S. and Chandiramani, N. K. (2011), "Optimal static output feedback control of a building using an MR damper", *Struct. Control Hlth. Monit.*, **18**(8), 852-868.
- Rodriguez, A., Ikhrouane, F., Rodellar, J. and Luo, N. (2009a), "Modeling and identification of a small-scale magnetorheological damper", *J. Intel. Mater. Syst. Struct.*, **20**(7), 825-835.
- Rodriguez, A., Iwata, N., Ikhrouane, F. and Rodellar, J. (2009b), "Model identification of a large-scale magnetorheological fluid damper", *Smart Mater. Struct.*, **18**(1), 015010.
- Schurter, K.C. and Roschke, P.N. (2000), "Fuzzy modeling of a magnetorheological damper using ANFIS", *The Ninth IEEE International Conference on Fuzzy Systems*.
- Sobel, K., Kaufman, H. and Mabus, L. (1982), "Implicit adaptive control for a class of MIMO systems", *IEEE Tran. Aerosp. Elec. Syst.*, **18**(5), 576-590.
- Spencer Jr, B., Suhardjo, J. and Sain, M. (1994), "Frequency domain optimal control strategies for aseismic protection", *J. Eng. Mech.*, **120**(1), 135-158.
- Spencer, B., Dyke, S., Sain, M. and Carlson, J. (1997a), "Phenomenological model for magnetorheological dampers", *J. Eng. Mech.*, **123**(3), 230-238.
- Spencer, Jr, B., Carlson, J.D., Sain, M. and Yang, G. (1997b), "On the current status of magnetorheological dampers: Seismic protection of full-scale structures", *Proceedings of the American Control Conference*.
- Spencer, Jr, B., Christenson, R.E. and Dyke, S. J. (1998a), "Next generation benchmark control problem for seismically excited buildings", *Proceedings of the Second World Conference on Structural Control*.
- Spencer, Jr, B.F., Yang, G., Carlson, J.D. and Sain, M.K. (1998b), "Smart dampers for seismic protection of structures: a full-scale study", *Proceedings of the Second World Conference on Structural Control (2WCSC)*, Kyoto, Japan.
- Spencer, Jr, B. and Nagarajaiah, S. (2003), "State of the art of structural control", *J. Struct. Eng.*, **129**(7), 845-856.
- Tsang, H.H., Su, R.K.L. and Chandler, A.M. (2006), "Simplified inverse dynamics models for MR fluid dampers", *Eng. Struct.*, **28**(3), 327-341.
- Vadtala, I.H., Soni, D.P. and Panchal, D.G. (2013), "Semi-active control of a benchmark building using neuro-inverse dynamics of MR damper", *Procedia Eng.*, **51**, 45-54.
- Yoshida, O. and Dyke, S.J. (2004), "Seismic control of a nonlinear benchmark building using smart dampers", *J. Eng. Mech.*, **130**(4), 386-392.
- Zhang, Z.Y., Huang, C.X., Liu, X. and Wang, X.H. (2011), "A novel simplified and high-precision inverse dynamics model for magneto-rheological damper", *Appl. Mech. Mater.*, **117-119**, 273-278.
- Zong, L.H., Gong, X.L., Guo, C.Y. and Xuan, S.H. (2012), "Inverse neuro-fuzzy MR damper model and its application in vibration control of vehicle suspension system", *Veh. Syst. Dyn.*, **50**(7), 1025-1041.